

1 Introduction

Having profound effects on the evolution of stars and their surroundings, the study and understanding of stellar winds is of great importance in modern astrophysics. Toward this end, observations must be carried out and models must be advanced. In the present text, emphasis will be given to the concept of observational methods, in particular the interpretation of the so-called P Cygni line profile, and the main effects the resulting mass loss.

2 Observations of stellar winds

2.1 Fundamental concepts

Observations of the stellar winds provide us with a direct test of our models. Several parameters can be derived from observations; among these, the two most important are the *rate of mass loss* \dot{M} and the *terminal velocity* v_∞ , i.e. the velocity of the stellar wind at a large distance from the star. For a star like our Sun, $\dot{M} = 10^{-14} M_\odot \text{ yr}^{-1}$, whereas massive stars easily reach $\dot{M} = 10^{-6} M_\odot$. Typical values for v_∞ range from $\sim 10 \text{ km s}^{-1}$ for cool supergiants to 3500 km s^{-1} for early-type stars (Cassinelli, 1992).

As \dot{M} describes the amount of material lost by the star per unit time, it is important for the evolution of the star, because stars with high mass loss rates evolve differently from those with low mass loss rates.

Different theories predict different values for \dot{M} and v_∞ , so by comparing observations with predictions we can learn which mechanisms are responsible for the winds.

The mass loss not only affects the star. It also enriches the interstellar medium with various elements and carries away kinetic energy, depositing an amount of $\frac{1}{2}\dot{M}v_\infty$ per unit time into its surroundings.

2.1.1 The equation of mass continuity

Although not being the case for a large number of stars, in our approach we will assume spherical symmetry. This will serve as a foundation for dealing with the more difficult problems of distorted stars. Thus, we have the *equation of mass continuity*

$$\dot{M} = 4\pi r^2 \rho(r)v(r), \quad (1)$$

where r is the distance from the center of the star, ρ is the density and v is the velocity. The equation is merely a form of Kirchhoff's 2nd law, stating that matter is neither created nor destroyed in the wind.

2.1.2 The velocity law

When the gas leaves the photosphere, its radial velocity v_0 is typically less than 1 km s^{-1} . It is then gradually accelerated until at a very large distance from the star, the velocity asymptotically approaches v_∞ . The *velocity law* $v(r)$ describes the distribution of the velocity of the wind with r . Observations and models of stellar wind indicate that $v(r)$ often can be approximated by a β -law, which varies as

$$v(r) \simeq v_0 + (v_\infty + v_0) \left(1 - \frac{R_\star}{r}\right)^\beta, \quad (2)$$

where R_* is the radius of the star, and the parameter β describes how steep the velocity law is. Winds from hot star experience a fast acceleration and may have $\beta \simeq 0.8$, whereas winds from cool stars accelerate more slowly, and hence have larger values of β . (Lamers and Cassinelli, 1999).

2.1.3 Line formation

As a consequence of the large velocities involved, spectral lines from stellar winds are somewhat broadened, and thus easy to distinguish from photospheric lines. The lines are formed in a number of different ways:

Photons created in the photosphere are scattered on the atoms in the wind. Scattering is most important for transitions of low excited levels because the life time for spontaneous de-excitation is small. In particular, resonance lines are often observed in stellar winds.

Colliding ions and electrons in the wind produce recombination lines; most likely from recombining directly to the ground state of the ion, but also to an excited level and then cascading downwards. The $H\alpha$ emission and IR emission in hot stars is due to this process.

Kinetic energy of the gas is converted into line photons by collisions and subsequent de-excitation. This process is most efficient in hot plasmas, and is responsible for the formation of emission lines from hot chromospheres and coronae.

In addition to the above there is masering by stimulated emission and, of course, pure absorption. The former will only be significant in the winds of cool stars where the velocity gradient is small, so that the process is not inhibited by a Doppler shift. The latter will not be important in stellar winds because the vast majority of atoms are in their ground state, and thus the only significant absorption will be considered as scattering.

2.2 P Cygni profiles

The most direct observational evidence for the presence of a stellar wind is the P Cygni line profile. Qualitatively, this profile consists of the sum of an absorption component due to the gas between the star and the observer, blue-shifted because of the motion of the gas, and an emission component from light scattered on the expanding envelope, with both negative and positive velocities relative to the observer. A P Cygni profile is shown in fig. 1.

If the stellar wind cannot be assumed optically thin to line radiation, the problem of

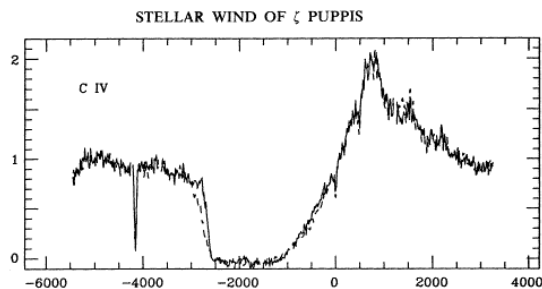


Figure 1: The P Cygni profile of the C IV line in the spectrum of ζ Puppis, an O4I(n)f star. The profile extend to $v \simeq -2700 \text{ km s}^{-1}$ (from Prinja *et al.*, 1992).

radiative transfer in the moving medium would be ghastly. Fortunately, as first realized by Sobolev (1958), the velocity gradient of the expanding gas effectively makes all points move away from each other. As a result, as soon as a line photon has traveled a small distance, it is Doppler shifted with respect to the surrounding gas and can no longer be absorbed by the same line transition

To understand the shape of a P Cygni line profile, we first consider isotropic scattering of stellar photons in a geometrically and optically thin shell centered on the star at distance between r and $r + \Delta r$ with corresponding expansion velocity between v and $v + \Delta v$. Referring to fig. 2a, the part of the shell from $-\theta$ and $+\theta$, where $\sin \theta = R_*/r$, will lie between the star and the observer and thus remove some of the photons by scattering that would have otherwise reached the observer. As seen by the atom, the stellar photons are red-shifted, so it needs a more energetic photon to produce a given line. Hence, this will result in a narrow blue-shifted absorption component, extending from Doppler velocity $-v$ to $-v \cos \theta$.

In turn, photons can be scattered in the direction of the observer from the whole shell, save the part that is occulted by the star. This gives rise to an emission component extending from $-v$ to $+v \cos \theta$

Integrating all shells and summing absorption and emission gives the observed P Cygni

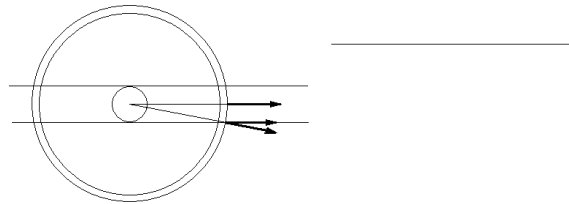


Figure 2: Left: The geometry of one shell of expanding gas around the star. Right: The same shell's contribution to the total absorption and emission, where the emission between $+v \cos \theta$ and $+v$ has been truncated by the occultation of the star.

profile, as indicated in fig. 3.

In the above discussion, the intrinsic broadening by thermal motions in the wind has

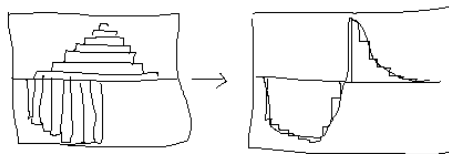


Figure 3: Left: Contributions to absorption and emission from all shells. Right: The resulting P Cygni profile is a sum of all the contributions.

been neglected. This will be safe for all but the slowest stellar winds.

2.3 Determination of mass loss and velocity law from P Cygni profiles

The velocity law and v_∞ can be derived most accurately from the profiles of saturated lines which have a steep blue absorption edge. This will reach the continuum at a Doppler velocity of $v_{\text{edge}} \simeq -(v_\infty + 2v_{\text{turb}})$, where v_{turb} is the turbulence velocity of the gas at a distance of $r \gtrsim 10R_\star$, where v_∞ is reached (Lamers and Cassinelli, 1999) (see fig. 1).

Comparing observed and predicted unsaturated P Cygni line profiles for different radial distributions $n_i(r)$ of the observed ions in the wind, it is possible to derive the mass loss. When the profiles match one another, the ion density $n_i(r)$ is known. If the abundance $A_e = n_e/n_H$ of the element with respect to hydrogen and the ionization fraction $q_i = n_i/n_e$ of the observed ion is known, $n_i(r)$ can be converted into a density distribution $\rho(r)$ and then, by means of eq. (1) into an expression for \dot{M} :

$$\begin{aligned} n_i(r) &= \frac{n_i(r)}{n_e(r)} \frac{n_e(r)}{n_H(r)} \frac{n_H(r)}{\rho(r)} \rho(r) \\ &= q_i(r) A_e \frac{n_H(r)}{\rho(r)} \frac{\dot{M}}{4\pi r^2 v(r)}, \end{aligned}$$

or

$$\dot{M} = 4\pi r^2 v(r) \frac{n_i}{q_i A_e (n_H/\rho)}. \quad (3)$$

The ratio n_H/ρ depends on the composition of the wind and is $(1.36m_H)^{-1} = 4.43 \times 10^{23}$ atoms g^{-1} for solar composition (*ibid*).

2.4 Alternative observational methods

Although the above approach is often the best, several other methods for determining \dot{M} and v_∞ , as well as other parameters, exist. Stars with high mass loss rates may show emission lines from the wind in their spectra. Stars with an ionized stellar wind emit an excess of continuum emission at long wavelengths, due to free-free emission (Bremsstrahlung) from the wind. Cool stars emit molecular emission lines, and may even have an excess in IR and mm wavelengths due to dust. From the information one gets from these spectra, one can also derive the mass loss and terminal velocity.

3 The effects of mass loss on stellar evolution

Depending on the initial mass M_i of a star, the loss of mass will affect the star differently. In the case of very massive stars ($M_i \gtrsim 30M_\odot$), mass loss occurs at a considerable rate through their whole life, affecting their evolution from life to death. For lower mass stars, mass loss is only important in the late stages of their evolution. Below some of the main effects of mass loss is described.

3.1 Changes in surface composition

If convection occurs in the star's interior, the products of nuclear burning will be mixed with the original material throughout the convective region. When the outer layers are peeled off by mass loss, these products appear at the surface of the star, resulting in drastic changes in the abundances of the chemical elements in the stellar photosphere. In this way

an initially O-rich low mass star can exhibit a C-rich atmosphere on the asymptotic giant branch. The mass loss also explains the ON stars, which are early type stars with a high N and a low C abundance, whereas the star originally had a higher C than N abundance. Moreover, it offers an explanation of the Wolf-Rayet stars, which have a high abundance of He and a low abundance of H at their surface. WN stars have a high N surface abundance due to the products of the H-burning via the CN cycle, and WC stars have a high C surface abundance due to the products of He-burning.

3.2 Changes in the luminosity and main sequence lifetime

As the luminosity L of a star depends strongly on its mass during core H-burning, massive stars suffering high mass loss already during their main sequence phase will have a smaller L than a star with the same M_i but without mass loss, thus extending its MS lifetime. de Loore *et al.* (1978) have calculated the MS lifetimes for stars of varying M_i 's and \dot{M} 's and find, e.g., that whereas a star of $M_i = 30 M_\odot$ with no mass loss spends 4.0 Myr on the MS, stars with mass losses of¹ $\dot{M} = 100L/c^2$ and $\dot{M} = 300L/c^2$ spend only 4.8 Myr and 5.6 Myr, respectively, leaving the MS with masses of $25.6 M_\odot$ and $18.2 M_\odot$, respectively.

3.3 The lack of luminous red supergiants

At the end of their core H-burning phase, stars develop a convective outer envelope, thus expanding their radius and moving to the right in the Hertzsprung-Russell diagram. When mass loss has decreased the mass of the H-rich outer zone below some critical minimum, this envelope can no longer be in convective equilibrium but contracts into a thinner envelope in radiative equilibrium. This results in a decrease in the stellar radius and a blueward motion of the star in the HR diagram. The most massive stars lose so much mass during their MS phase and shortly thereafter as luminous blue variables that their envelopes have insufficient mass to become convective, so these stars cannot become red supergiants. This explains the lack of red supergiants brighter than about $L \sim 5 \times 10^5 L_\odot$ (Lamers and Cassinelli, 1999).

3.4 The formation of planetary nebulae

In the asymptotic giant branch phase, stars with $M_i \lesssim 8 M_\odot$ suffer severe mass loss, resulting in a large amount of circumstellar material expanding with a velocity of about 10 km s^{-1} . When the remaining H-envelope has insufficient mass to sustain a large convective envelope, the star contracts, moving to the left in the HR diagram. When $T_{\text{eff}} \gtrsim 30\,000 \text{ K}$, the radiation ionizes the circumstellar material. At the same time the star starts to blow a fast low density wind that interacts with the slow high density wind from the AGB phase, resulting in a planetary nebula.

3.5 The formation of white dwarves

When a star ends its life, its fate depends on its final mass M_f . If $M_f < 1.4 M_\odot$ it becomes a white dwarf; otherwise it will explode as supernova that leaves behind a neutron star

¹On the basis of the empirically found relation for the mass loss rate of supergiants and evolved O stars indicating that the rate is nearly always proportional to the luminosity (Barlow and Cohen, 1977), de Loore *et al.* parametrize the mass loss by $\dot{M} = NL/c^2$, where c is the speed of light and observed mass loss rates correspond to about $N = 100 \pm 50$ (*ibid.*).

or a black hole. The presence of white dwarves in clusters with a MS turn-off mass of up to 6 or 8 M_{\odot} indicate that white dwarves can be formed from stars with initial masses this high. In order not to explode as supernovae, these star must have lost a considerable fraction of their mass during their late evolution phases.

4 Literature

Barlow, M. J., Cohen, M., 1977, *Infrared photometry and mass loss rates for OBA supergiants and Of stars*, A & A 213, p. 737.

Cassinelli, J.P., 1992, in *The Astronomy and Astrophysics Encyclopedia* (ed. S.P. Maran), Cambridge University Press, p. 809.

de Loore, C., de Grève, J. P., Vanbeveren, D., 1978, *Parameters of Massive Stars of Main Sequence Evolution without and with Stellar Wind*, A & A Suppl. 34, p. 363.

Lamers, H.J.G.L.M. & Cassinelli, J.P., 1999, *Introduction to stellar winds*, Cambridge University Press.

Prinja, R. K., 1992, Balona, L. A., Bolton, C. T., Crowe, R. A., Fieldus, M. S., Fullerton, A. W., Gies, D. R., Howarth, I. D., McDavid, D. & Reid, A. H. N., *Time series observations of O stars. I - IUE observations of variability in the stellar wind of Zeta Puppis*, A & A 390, p. 266.

Sobolev, V.V., 1958, *The Formation of Emission Lines*, Theoretical Astrophysics (ed. V.A. Ambertsumyan, trans. J.B. Sykes), Pergammon, New York.